Chapter 5
Prestin: Molecular Mechanisms Underlying Outer Hair Cell Electromotility

Joseph Santos-Sacchi, Dhasakumar Navaratnam, Rob Raphael, and Dominik Oliver

Abstract Prestin is a member of the SLC26 family of anion transporters that has evolved to serve as a molecular motor in outer hair cells (OHCs) of the mammalian inner ear. The protein is piezoelectric-like, exhibiting voltage and tension sensitivity, with significant modulation by anions, chiefly intracellular chloride. Receptor potentials of OHCs drive molecular conformational changes in prestin, as evidenced by voltage sensor charge movements, that evoke robust length changes in OHCs, thereby contributing to a mechanical feedback mechanism and, therefore, to cochlear amplification, which enhances our auditory sensitivity. Current research has been focused on tertiary structural determinations, prestin interactions with other proteins and membrane lipids, trafficking, and the mechanism of anion effects. One of the key remaining questions is the determination of structural changes induced by membrane voltage perturbations and how those changes result in forces exerted by the OHCs. Indeed, much remains to be understood about this extraordinary molecule.

J. Santos-Sacchi (✉)
Departments of Surgery (Otolaryngology), Neuroscience, and Cellular
and Molecular Physiology, Yale University School of Medicine, 333 Cedar Street,
New Haven, CT 06520-8018, USA
e-mail: joseph.santos-sacchi@yale.edu

D. Navaratnam
Departments of Neurology and Neuroscience, Yale University School of Medicine,
333 Cedar Street, New Haven, CT 06520-8018, USA
e-mail: dhasakumar.navaratnam@yale.edu

R. Raphael
Department of Biomedical Engineering, Rice University, 6100 Main Street,
Houston, TX 77521, USA
e-mail: rraphael@rice.edu

D. Oliver
Department of Neurophysiology, Philipps-Universität Marburg,
Deutschhausstrasse 2, 35037 Marburg, Germany
e-mail: oliverd@staff.uni-marburg.de

5.1   Introduction

Prestin is a remarkable protein that underlies our keen sense of hearing. It is a member of an anion transporter family (SLC26) that has role changed into a fast molecular motor that drives outer hair cell (OHC) somatic electromechanical activity, the transduction of the receptor potential of the cell (see Corey, Ó Maoiléidigh, and Ashmore, Chap. 4) into pronounced cell length changes at acoustic rates, thereby boosting perceptual thresholds by 40–60 dB. In this chapter, three broad areas focus on how this protein works. They include an overview of the protein's biophysical traits, the structural features of the protein that will lead to detailed structure-function relationships, and the role of accessory protein/lipid partners in helping this protein to carry out its important work. Much is to be learned. Pertinent reviews on the subjects of this chapter are available in the literature (He et al. 2006; Ashmore 2008; Ashmore et al. 2010).

5.2   Known Biophysical Properties of Prestin

5.2.1   The OHC Sensor/Motor: Preprestin

An intense investigation of this somatic motility began soon after its discovery by Bill Brownell and colleagues (Brownell et al. 1985; Kachar et al. 1986). Surprisingly, when OHCs are stimulated electrically by a current injection within or across the cell, their length changes as a function of stimulus intensity and waveform. It soon became clear that OHC somatic motility [also known as electromotility (eM)] was driven by voltage and not any particular ionic current (Ashmore 1987; Santos-Sacchi and Dilger 1988), evidencing movements of 15 nm/mV on average (Santos-Sacchi 1989). One of the most powerful pieces of evidence that eM was driven by voltage was the observation of displacement currents, capacitive-like currents, similar in some respects to the gating currents of ion channels (Bezanilla 2000), which are evoked by membrane voltage steps under whole cell voltage clamp (Ashmore 1989; Santos-Sacchi 1990). These displacement currents, or, equivalently, a voltage-dependent or nonlinear membrane capacitance (NLC), arise from the movements of a voltage sensor charge across the electric field of the membrane. The identification of such a charge movement immediately led to the notion of a sensorimotor unit residing in the OHC plasma membrane that obeyed

two-state Boltzmann statistics (Ashmore 1990; Santos-Sacchi 1991), where characterization of the charge-voltage (Q-V) or, equivalently, the capacitance-voltage (C-V) relationship provides estimates of the unitary sensor charge (z; assuming full passage of the sensor charge through the field of the membrane), the maximum charge transferred (Q_{max}), and, the voltage where charge is equally distributed across the membrane (V_h; Fig. 5.1). The Boltzmann characterization of motor charge movement also provided the impetus for the development of "molecular" models of motor action that incorporated Boltzmann statistics, including area and conformational state models (Kalinec et al. 1992; Dallos et al. 1993; Iwasa 1994). Given the Q_{max} and an elementary sensor charge estimate, the number of motors residing in the membrane can be estimated, giving a density in OHCs of about $10,000/\mu m^2$ (Huang and Santos-Sacchi 1993; Gale and Ashmore 1997a; Mahendrasingam et al. 2010), although this number may need to be reevaluated (Santos-Sacchi and Song 2016). V_h and z have been used to define the voltage operating range of the motor, with V_h localizing the eM-V function relative to the resting membrane potential of the cell and z defining the extent over which the motor is voltage sensitive. With z being less than unity, the motor has a quite shallow voltage dependence compared with ion channels. The two-state formalism also imposes strict correspondence between charge movement and eM, where according to a now widely accepted area-state model (Iwasa 1994; Santos-Sacchi and Song 2014a), motors will fluctuate between a compact and expanded surface area state, with unitary motor area change estimates varying between 0.37 and 8 nm^2 (Iwasa 1993; Santos-Sacchi 1993; Gale and Ashmore 1994; Adachi and
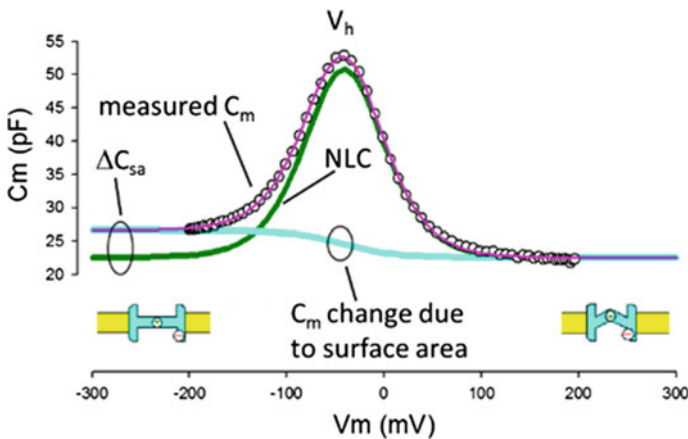

Fig. 5.1 Outer hair cell (OHC) nonlinear membrane capacitance (NLC). OHC voltage-dependent capacitance (*circles*) is composed of two components, both riding atop a linear capacitance corresponding to the cell's surface area. One is associated with the voltage sensor charge of prestin (NLC; *green*), and the other is associated with motor state occupancy (*blue*). Cartoon depicts prestin in either state, expanded or contracted. V_h, voltage where charge is equally distributed across the membrane; C_m, membrane capacitance; ΔC_{sa}, state-dependent capacitance; V_m, membrane voltage. See text for further details. Modified from Santos-Sacchi and Navarrete (2002)

Iwasa 1999). As indicated in Fig. 5.1, voltage-dependent C_m possesses an additional component, state-dependent capacitance (ΔC_{sa}), that has been attributed to area/membrane thickness changes associated with motor state occupancy, each motor contributing an additional 17 aF when residing in the expanded state (Santos-Sacchi and Navarrete 2002). The high variance of area estimates highlights the need for structural observations at the molecular level.

During the ensuing years, a host of biophysical attributes of the OHC plasma membrane motor were characterized, and these traits, together with its NLC, would be crucial in identifying the molecular nature of the motor. One of the most important discoveries was the piezoelectric nature of the motor (Iwasa 1993). On introducing tension into the OHC membrane, NLC shifts along the voltage axis. The shift in V_h effects the charge movement in the membrane, and this phenomenon is intrinsic to the membrane (Gale and Ashmore 1994; Kakehata and Santos-Sacchi 1995). These data are fully consistent with a direct voltage-to-mechanical (and vice versa) transduction process that does not directly require any intermediate steps (e.g., second messengers) or biochemical energy sources (except, of course, those sources required to maintain the membrane voltage). Other early observations that defined the nature of the motor and set the stage for its molecular identification included the simultaneous block of the NLC and motor activity by intracellularly acting salicylate and extracellularly acting gadolinium (Santos-Sacchi 1991; Tunstall et al. 1995; Kakehata and Santos-Sacchi 1996), the influence of altered membrane potential (prepulse effect) on V_h (Santos-Sacchi et al. 1998), the tension and turgor pressure effects (piezoelectric-like) on the NLC (Iwasa 1993; Gale and Ashmore 1994; Kakehata and Santos-Sacchi 1995), and the temperature susceptibility of the NLC (Santos-Sacchi and Huang 1998; Meltzer and Santos-Sacchi 2001).

5.2.2 Enter Prestin

Zheng et al. (2000) identified the OHC motor protein as prestin (SLC26A5), a member of an anion transporter family. Key to this identification was the localization of the protein to the OHC lateral membrane where electromechanical activity is restricted (Dallos et al. 1991; Huang and Santos-Sacchi 1994) and biophysical demonstrations of OHC motor-like activity in heterologously transfected cells, including the NLC, the voltage-driven membrane movement, and a block by salicylate. Subsequently, prestin was shown to exhibit membrane tension (Ludwig et al. 2001; Santos-Sacchi et al. 2001), prepulse (Santos-Sacchi et al. 2001), and temperature sensitivities similar to those in the native OHCs (Meltzer and Santos-Sacchi 2001). It was clear at that point that all known biophysical traits of prestin matched those that had been identified before its discovery. Another fundamental observation that indisputably linked prestin to OHC eM was the absence of eM in the prestin-knockout mouse (Liberman et al. 2002).

5.2.3   Importance of Prestin for Cochlear Amplification

Interestingly, while the knockout implicated the importance of prestin in cochlear amplification, issues were quickly identified that dampened such a conclusion, including the obvious mechanical impedance changes in the OHCs (and consequently the cochlear partition) that result from removal of the abundant protein content within the OHC lateral membrane, which substantially shortened OHCs. Subsequently, persuasive evidence that prestin predominantly underlies cochlear amplification was obtained from a knockin of mutated prestin (499 mutant) that has its voltage operating range (assessed by NLC V_h) shifted far out of the physiological range while maintaining other features of normal OHC function, structure, and mechanics (Dallos et al. 2008). That mutation also altered the kinetics of prestin (Homma et al. 2013). Another important observation linking prestin to cochlear amplification was that manipulations of chloride, previously shown to control the electromechanical activity of prestin (Oliver et al. 2001), reversibly altered the basilar membrane tuning in vivo (Santos-Sacchi et al. 2006). Salicylate, which competes with chloride for the anion binding site of prestin and reduces the NLC (Oliver et al. 2001), also adversely affects basilar membrane motion (Santos-Sacchi et al. 2006; Fisher et al. 2012). Finally, there is evidence for prestin mutations causing deafness (Mutai et al. 2013).

5.2.4   How Does Prestin Sense Voltage?

The voltage-dependent nature of eM naturally begs the question, What makes the protein sensitive to voltage? It is clear that prestin must possess a charged voltage sensor that is moved by voltage drops across the plasma membrane. In other well-studied voltage-dependent membrane proteins, charged amino acid residues serve this function. For example, the S4 segment in the voltage sensor domain of all classical voltage-gated ion channels comprises the voltage sensor domain (Bezanilla 2000). In a fundamental study investigating this issue, Oliver et al. (2001) found that neutralization of candidate electrically charged amino acid residues had little effect on voltage sensitivity of prestin, whereas removal of monovalent intracellular anions, namely intracellular chloride or bicarbonate, abolished charge movement and hence voltage sensitivity. Recently, careful examination of this phenomenon indicated that the OHC eM magnitude (Song and Santos-Sacchi 2013) and the total Q_{max} (Santos-Sacchi and Song 2016) do not decrease with intracellular chloride level, but rather chloride levels influence the rate of prestin transitions (Santos-Sacchi and Song 2016), resulting in an apparent reduction of NLC when the membrane potential is changed at rates exceeding the Cl^--dependent kinetics of prestin. Based on the observation of anion sensitivity, Oliver et al (2001) concluded that the voltage sensor of prestin is not made up from intrinsic residues in prestin, but instead, monovalent anions serve as extrinsic voltage sensors, i.e., that

charge movements (NLC) arise directly from the translocation of the anion across the electrical field along some hypothetical access channel in the protein. This anion translocation, in turn, would then drive simultaneous conformational changes between the expanded and contracted states, thus producing eM. In fact, the voltage dependence of prestin varied with the size of the monovalent anion present, as if bulkier anions can travel a smaller fraction of the electrical field (Oliver et al. 2001). However, other findings are difficult to reconcile with this simple external voltage sensor model. First, a shift of the voltage dependence (V_h) toward depolarized potentials observed when the anion concentration is lowered is contrary to the prediction of the model (Rybalchenko and Santos-Sacchi 2003a). Interestingly, a variety of anion substitutes can markedly shift V_h in either the depolarizing or hyperpolarizing direction to varying degrees (Oliver et al. 2001; Rybalchenko and Santos-Sacchi 2008). Second, if other than monovalent anions can maintain prestin function, the charge number z moved per prestin molecule should correspond to the valence of the anion serving as voltage sensor (assuming that the electrical distance traveled remains the same). However, an increase in z has not been observed when monovalent anions are substituted with di- or trivalent anions (Rybalchenko and Santos-Sacchi 2008). Third, hyperpolarization, which drives prestin into the expanded state, should move the anion toward a more extracellular position, but in the expanded state, the apparent affinity for the anions is reduced, suggesting the release toward the cytosol (Song and Santos-Sacchi 2010). Observations such as these have led to a counter theory that anions serve as allosteric-like modulators of prestin charge movement, anion binding conformationally transitioning the protein into a voltage-enabled state, with sensor charge contributed by a wide-ranging distribution of charged residues within the protein (Bai et al. 2009). A current structural view of anion interaction with prestin is provided in Sects. 5.3.4 and 5.3.5.

5.2.5 How Many States/Transitions Does Prestin Have?

Simply based on standard fits of the NLC, it was not possible to differentiate between two-state and multistate behavior in the motor protein prestin (Huang and Santos-Sacchi 1993; Scherer and Gummer 2005). For example, fits with two-state Boltzmann or infinite state Langevin equations each adequately fit the NLC because of measurement uncertainty at the extreme voltages needed to interrogate the very shallow voltage dependence of the protein. The NLC has been used routinely as a surrogate for eM under the assumption that sensor charge movement exhibits fast two-state behavior directly linked to eM. It was natural to assume such fast kinetics because eM had been measured in the acoustic frequency range (Ashmore 1987; Santos-Sacchi 1992; Dallos and Evans 1995), even out to about 80 kHz (Frank et al. 1999) at room temperature. Interestingly, the NLC cutoff frequency was near 10 kHz at room temperature (Gale and Ashmore 1997b). The recent observation that characteristics of the NLC and eM can diverge as a function of reduced anion

concentration revealed that prestin activity is not governed by a simple two-state process but is instead multistate (Song and Santos-Sacchi 2013). A basis for disparity between the two measures may be related to slow, chloride-controlled intermediate transitions between chloride-binding and voltage-enabled states (Song and Santos-Sacchi 2013; Santos-Sacchi and Song 2014a). Essentially, steady-state (or low-frequency) evaluations of eM do not correspond to sensor charge movement that is measured at higher frequencies because each will only be equal when measured at the same frequency. Although the simple model developed in that work (*meno presto* model) can recapitulate features of the behavior of prestin, thus revealing its multistate nature with attendant time/phase delays (Santos-Sacchi and Song 2014b), it is likely that models incorporating transporter characteristics expected from the SLC heritage of prestin will offer greater insight (Muallem and Ashmore 2006; Schaechinger et al. 2011), provided they can account for all known biophysical properties exhibited by prestin.

Clearly, a lack of consensus on the structure of prestin based on software prediction algorithms, as indicated by the wide range of secondary topologies attributed to the membrane protein such as the 12 transmembrane domain (TMD) model (Oliver et al. 2001; Deak et al. 2005; Rajagopalan et al. 2006), the 10 TMD model (Navaratnam et al. 2005), and the 8 TMD model (Lovas et al. 2015), has led to difficulties in understanding the biophysical basis of the NLC and eM. Additionally, the limited information on the interacting partners of prestin and the influence of its membrane environment has contributed to these difficulties. Fortunately, significant progress is currently being made on these fronts.

5.3 Structure and Function of Prestin

5.3.1 Molecular and Functional Features of Prestin

Prestin is the fifth member of the SLC26 family of anion exchangers (hence SLC26A5; Zheng et al. 2000), a group of 10 mammalian proteins (Mount and Romero 2004; Alper and Sharma 2013). SLC26 proteins belong to a large, ubiquitous, and evolutionarily ancient "sulfate permease" (SulP) family of anion transporters present in animals, plants, fungi, and bacteria. Although the SLC26 nomenclature was originally used for the mammalian SulP proteins (Mount and Romero 2004), the SulP and SLC26 nomenclature may be used interchangeably (Dorwart et al. 2008; Geertsma et al. 2015). These evolutionary and molecular relationships are of particular relevance because structural information on mammalian prestin has emerged only very recently and is entirely based on crystallographic data for close (i.e., within the SLC26/SulP family) or remotely homologous relatives of mammalian SLC26 proteins.

The mammalian SLC26 proteins are diverse in terms of both their transport substrates and the transport modes. Thus, SLC26 transport activities include

electrogenic or electroneutral exchange of monovalent (e.g., chloride, iodide) and divalent anions (e.g., sulfate, oxalate). Two members, SLC26A7 and SLC26A11, mediate uncoupled flux of chloride at high rates, which may indicate that these members function as anion channels. Detailed reviews on SLC26 transport function and roles in physiology and pathophysiology are available (Mount and Romero 2004; Dorwart et al. 2008; Alper and Sharma 2013).

The closest prestin relatives of mammalian prestin, nonmammalian orthologs of SLC26A5 (e.g., chicken and zebrafish prestin), are highly active anion transporters that mediate the stoichiometric exchange of monovalent anions such as chloride against divalent anions (either sulfate or oxalate; Schaechinger and Oliver 2007; Schaechinger et al. 2011). Because this transport mode is electrogenic, i.e., one electrical charge is transferred per transport cycle, nonmammalian prestins generate robust transport currents in the presence of divalent transport substrates (Schaechinger and Oliver 2007). In contrast, transport currents were not observed with mammalian prestin in the presence of divalents (Schaechinger and Oliver 2007; Schaechinger et al. 2011), indicating that prestin has no transport activity, that it acts in an electroneutral mode that does not generate electrical current, or that transport rates are much lower than in its nonmammalian orthologs. In fact, by using fluorescent pH sensors and electrophysiology, Mristik et al. (2012) showed that prestin may function as a Cl^-/ $2HCO_3^-$ exchanger, however with a low transport rate. Recently, prestin has been shown to allow ion currents through a pathway distinct from its transporter pathway (Bai et al. 2017). Moreover, based on a tracer-flux assay, one study suggested transport capability for formate and chloride (Bai et al. 2009), although another group could not reproduce this finding while confirming transport in nonmammalian orthologs (Tan et al. 2011). Interestingly, prestin, as well as other SLC26 proteins, mediates uncoupled permeation of thiocyanate (SCN^-) at appreciable rates (Schanzler and Fahlke 2012). Although the permeation of this anion has no obvious physiological relevance, this finding underscores the high degree of mechanistic and structural similarity between prestin and other SLC26 transporters and may turn out as helpful in deciphering potential common molecular mechanisms of transport and eM.

Mammalian prestin is a 744-amino acid protein with a high degree of sequence conservation across mammalian species (Zheng et al. 2000). As with other SLC26 proteins, prestin consists of a large TMD containing numerous hydrophobic stretches indicative of multiple transmembrane segments. This TMD is flanked by hydrophilic intracellular N- and C-termini (Ludwig et al. 2001; Zheng et al. 2001). The detailed topology of the TMD had long remained enigmatic, but it is now clear that it contains 14 membrane-spanning domains (Gorbunov et al. 2014; Geertsma et al. 2015). Within this TMD, two regions have been recognized for their particularly high sequence conservation across the SLC26/SulP family. One is located more N-terminally and is designated as the "SulP consensus signature" (Prosite PS01130); the other one located in the C-terminal half of the TMD is known as the Saier motif (Saier et al. 1999; Mount and Romero 2004). The high degree of conservation suggested that these protein regions are of particular importance for SLC26 function and may be critically involved in anion transport and possibly in eM. This is supported by the finding that transplantation of protein regions, including these motifs from mammalian prestin into

the prestin ortholog from zebrafish, is sufficient to confer mammalian-like function (i.e., fast charge transfer and eM) onto the nonmammalian prestin, which otherwise functions as a transporter (Schaechinger et al. 2011).

Another well-conserved domain of all mammalian and most bacterial SLC26/SulP proteins is the sulfate transporter and anti-sigma factor antagonist (STAS) domain, which occupies most of the cytoplasmic C-terminus (Sharma et al. 2011). The name refers to sequence and structural similarity with bacterial anti-sigma factor antagonist (ASA) proteins. In prestin from rats, the STAS domain approximately comprises amino acids 505–714 (Pasqualetto et al. 2010). Although the TMD mediates and determines the eM and transport function of SLC26 members as shown by transplantation of domains between mammalian and transport-active nonmammalian prestin (Schaechinger et al. 2011), mutagenesis studies indicated that the STAS domain is indispensable both for proper membrane targeting (Navaratnam et al. 2005; Zheng et al. 2005) and for protein function (Bai et al. 2006) in prestin and in other SLC26 transporters (Sharma et al. 2011). How the cytosolic domain affects eM or transport function is yet unknown. Nevertheless, as also found with other SLC26 transporters (Ko et al. 2004), the STAS domain is implicated in the interaction of prestin with other proteins including MAP1S (Bai et al. 2010) and calmodulin (Keller et al. 2014; see Sect. 5.4.2).

Although the prestin sequence is generally highly conserved across mammalian species, parallel or convergent evolution of the prestin gene has been discovered in echolocating bats and whales (Li et al. 2010; Liu et al. 2010). Thus, the same amino acid substitutions are found specifically in these phylogenetically unrelated lineages of echolocating mammals. Most of these sites cluster in the cytoplasmic C-terminus including the STAS domain (Li et al. 2010; Liu et al. 2010). Some of these residue replacements were found to modulate the voltage dependence of prestin (Liu et al. 2014), but the physiological consequences of these specific molecular traits are unknown. Given the parallel occurrence in echolocating species that use particularly high frequencies, it has been speculated that these amino acid changes may support the function of prestin in ultrasonic hearing (Li et al. 2010; Liu et al. 2010).

5.3.2   Molecular Structure of Prestin

Two papers in 2014 and 2015 revealed the molecular structure of SLC26/SulP transporters and of prestin in particular. Gorbunov et al. (2014) used a homology modeling approach based on the X-ray crystal structure of the bacterial uracil transporter UraA (Lu et al. 2011), which belongs to the NCS2 family of nucleobase/cation symporters, as the template. Although direct sequence conservation between UraA and prestin (or other mammalian SLC26 members) is low, advanced remote homology detection methods indicate that SLC26/SulP and NCS transporters are directly related, arguing that they share a common molecular architecture (Hoglund et al. 2011; Wong et al. 2012; Vastermark and Saier 2014). Homology models of mammalian and chicken prestin were scrutinized and refined

by molecular dynamics (MD) simulations (Gorbunov et al. 2014), which supported
the validity of this conclusion. Soon afterward, this homology model was confirmed
by the first experimental atomic structure of a SLC26/SulP transporter, the bacterial
fumarate transporter SLC26Dg from *Deinococcus geothermalis* (Geertsma et al.
2015).

Modeling and X-ray crystallography consistently revealed a 7 + 7
inverted-repeat architecture for the TMD of SLC26 transporters and thus prestin
(Gorbunov et al. 2014; Geertsma et al. 2015). As illustrated in Fig. 5.2, the central
domain (TMD) of prestin is made up of 14 mostly helical transmembrane
(TM) segments of variable length. The two halves (or repeats) of the TMD, each
containing seven TM segments, are related to each other by a twofold pseu-
dosymmetry such that they are inversely oriented with respect to the intracellular
side. TMs from both repeats are interdigitated with their counterparts from the other
repeat (Fig. 5.3a), forming the inverted-repeat organization that is characteristic of
many different transporters (Forrest and Rudnick 2009). The topology of prestin
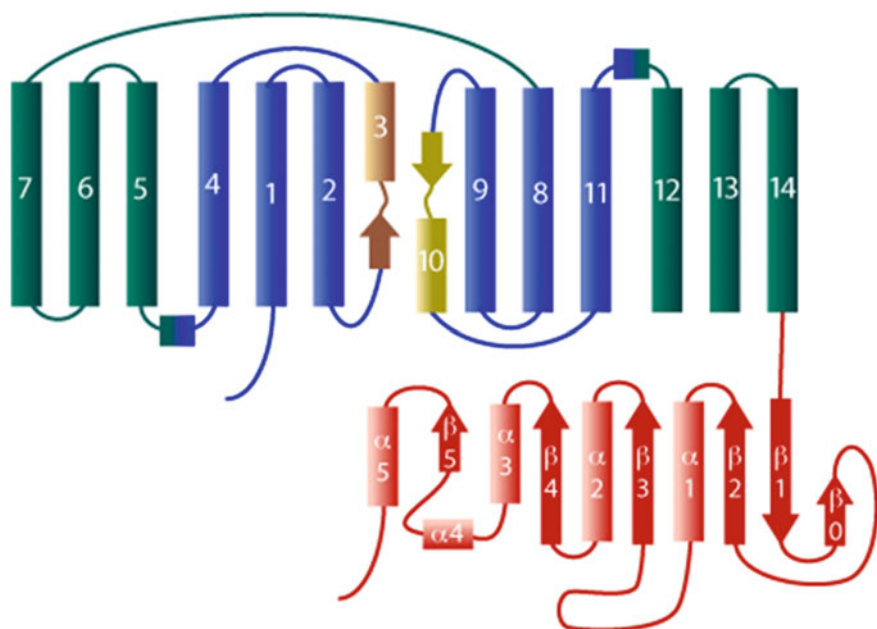was further probed by examining the intra- and extracellular accessibility of

Fig. 5.2 Topology of prestin. The transmembrane domain (TMD) contains 14 largely helical
membrane-spanning domains, forming two inverted repeats (TMs 1–7 and TMs 8–14). Colors
indicate the three-dimensional structural organization into two main helix bundles, the "core"
domain (*blue*) and the "gate" domain (*green*). Two central, partially helical and antiparallel TMs
within the core domain are highlighted in *brown* (TM3) and *yellow* (TM10). *Arrows*: short
β-strand segments. The cytoplasmic C-terminus (*red*) is mostly folded into a sulfate transporter
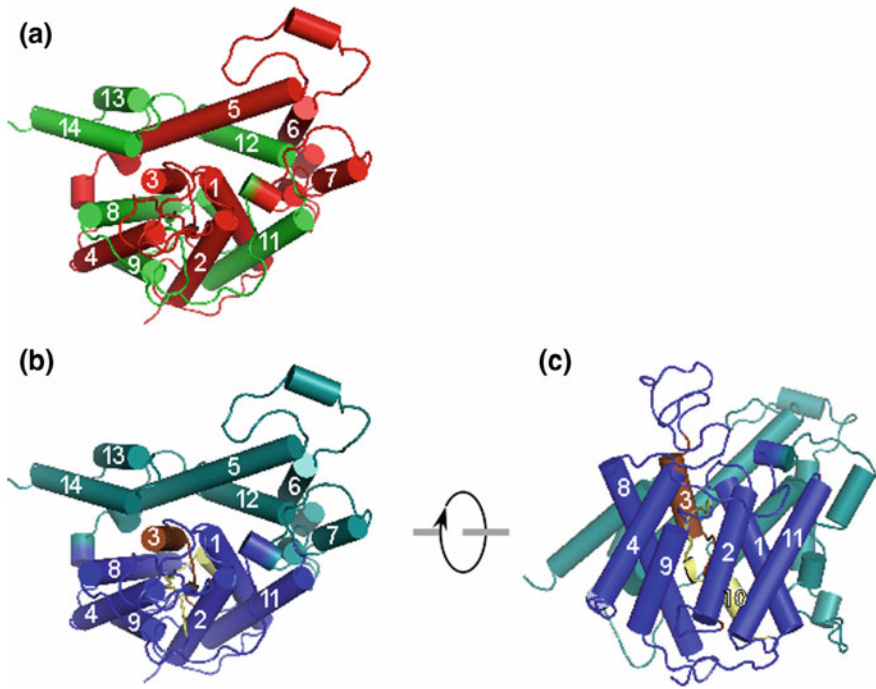and anti-sigma factor antagonist (STAS) domain consisting of several α-helical and β-strand
segments

Fig. 5.3 Three-dimensional structure of prestin. **a** Extracellular surface view of overall TMD structure of prestin as derived from homology modeling with the experimental structure of SLC26Dg (Geertsma et al. 2015) as the template. *Red*: inverted repeat I; *green*: inverted repeat II. Transmembrane segments are labeled as in Fig. 5.2; helical part of TM 10 is largely hidden by TM1. **b** Same structure colored according to structural organization in core and gate domain. Color code as in Fig. 5.2. **c** Side view

mutationally inserted cysteine residues to cysteine-reactive, membrane-impermeant reagents (Gorbunov et al. 2014). These experiments unequivocally showed that the topology of mammalian prestin is fully consistent with the architecture of the bacterial homolog and the homology model based on UraA.

The TMD is organized into two structural units, each consisting of a bundle of TM helices containing segments from both inverted repeats (Figs. 5.2, 5.3b, c). TMs 1–4 and the pseudosymmetry-related counterpart TMs 8–11 form a compact bundle that has been designated the core domain. TMs 5–7 and 12–14 fold into a more planar (extended) bundle of helices termed the gate domain, which aligns with one side of the core domain, forming an extensive interface between both domains (Fig. 5.3b).

Attempts were also made to address the molecular structure of SLC26A6 and prestin by homology modeling based on the crystal structures of a bacterial chloride transporter, CLC-ec1 (Ohana et al. 2011), or the bacterial amino acid transporter Glt$_{PH}$ (Lovas et al. 2015) as the templates, respectively. However, these approaches produced structures that can now be excluded given the lack of similarity with the

SLC26 crystal structure (Geertsma et al. 2015), disagreement with the experimentally determined topology (Gorbunov et al. 2014), and the lack of a sufficiently close evolutionary relationship between the respective transporter families and the SLC26/SulP family (Hoglund et al. 2011; Vastermark and Saier 2014).

The structure of the cytosolic STAS domain of prestin was solved at atomic resolution both for mammalian prestin (from the rat; Pasqualetto et al. 2010) and nonmammalian prestin (from the chicken; Lolli et al. 2015), revealing an ovoid domain assembled from a central β-sheet surrounded by five α-helices (Fig. 5.2). The core of the domain is structurally similar to STAS domains of bacterial SulP/LC26 proteins and to bacterial ASA proteins, but there are significant differences at the N- and C-termini, most notably an N-terminal extension including some rigid turns and an extra β-strand. Interestingly, the mammalian, but not the chicken, STAS domain harbors an anion binding site, the function of which is yet unknown (Lolli et al. 2015). Given its impact on prestin function, a close structural interaction with the TMD would seem likely. Although Pasqualetto et al. (2010) identified a molecular surface that may interact with either the lipid bilayer or the intracellular face of the TMD, the STAS orientation relative to the TMD remains unknown in the vertebrate SLC26 proteins. In the bacterial SLC26Dg full-length structure, the domain is facing away from the TMD and occupies a position corresponding to the inner lipid bilayer, which is apparently an artifact from cocrystallization with a nanobody (Geertsma et al. 2015). Low-resolution structural data from additional prokaryotic SLC26 homologs suggested that the STAS domain may project away from the TMD (Compton et al. 2014).

5.3.3 Oligomerization

Biochemical and low-resolution structural findings indicated that eukaryotic and bacterial SLC26 transporters share a conserved dimeric architecture (Detro-Dassen et al. 2008; Compton et al. 2011, 2014). However, some studies suggest that prestin forms tetramers (Zheng et al. 2006; Hallworth and Nichols 2012). Tetramers might be expected because particles in the lateral membrane of OHCs that are observed by freeze-fracture electron microscopy (EM) and believed to represent native prestin molecules, showed estimated diameters somewhat above 10 nm (Forge 1991; Kalinec et al. 1992). Given the dimensions of an SLC26 monomer of about 4.5 × 6 nm in the membrane plane (Gorbunov et al. 2014; Geertsma et al. 2015), these EM-resolved particles may correspond to tetrameric prestin assemblies. Also, a low-resolution structure of recombinant prestin, as obtained by a three-dimensional reconstruction based on single-particle EM images, exhibited four-fold symmetry consistent with tetrameric stoichiometry (Mio et al. 2008). It remains to be shown if these observations are due to the formation of higher order oligomers (i.e., dimers of dimers) and, if so, whether tetrameric assembly is important for functional or cell biological behavior.

The recent crystal structure of the bacterial SLC26Dg as well as the prestin homology structure provided no direct clues to the structural nature of dimerization. However, Geertsma et al. (2015) noted that the surface of the gate domain (opposite to the interface with the core domain) stood out due to high sequence conservation, which suggested that it may mediate dimerization. Interestingly, a recent crystal structure of the human anion exchanger AE1 (SLC4A1; also known as erythrocyte band 3 protein) showed that SLC4 transporters also share the 7 + 7 inverted-repeat architecture with SLC26 transporters, including an essentially superimposable arrangement of core and gate domains (Arakawa et al. 2015). This is consistent with the fact that together with the NCS2 family, the SLC4 family of bicarbonate transporters is one of the closest SulP/SLC26 relatives as indicated, e.g., by the Pfam database of protein families (Finn et al. 2014). This AE1 structure revealed a dimeric structure mediated by dimerization of the gate domains, lending support to a similar dimeric assembly of SLC26 proteins through the gate domains as proposed for SLC26 by Geertsma et al. (2015).

Although the mechanistic role of oligomerization in the transport or motor function of SLC26 proteins is unknown, for prestin it has been shown that subunits interact functionally, likely by an allosteric mechanism (Detro-Dassen et al. 2008). However, the atomic structure revealed the complete anion binding site and putative translocation pathway within the monomeric subunit (see Sect. 5.3.4), indicating that each subunit is basically functioning as an independent unit rather than forming an oligomeric common transport or motor domain with the other subunit.

5.3.4 Anion Binding Site

The SLC26/prestin structures provided a fresh mechanistic view into the anion dependence of the electromotile activity of prestin and the relationship to the transport function of related SLC26 proteins. Thus, the SLC26 structures feature a central cavity in the TMD, located halfway through the membrane and close to the interface between the core and gate domains. In both computational and X-ray structures, this cavity is accessible to solutes from the cytoplasm but is occluded from the extracellular space. Structural considerations and experimental evidence indicate that this central cavity is the principal binding site for the transport substrate in SLC26 transporters and specifically for the anion that enables eM in mammalian prestin. The pocket is formed largely by the two complementary pseudosymmetry-related, partially helical TMs 3 and 10 and by two complementary TM helices 1 and 8 (Fig. 5.4). Notably, these regions overlap with the Saier motif comprising TMs 9 and 10 (Saier et al. 1999; Mount and Romero 2004; Gorbunov et al. 2014), consistent with the high functional importance of this protein region as suggested by sequence conservation. Moreover, two protein regions previously recognized as molecular determinants of electromotile capability in prestin (Schaechinger et al. 2011) largely coincide with the domains forming the central pocket, further emphasizing the functional importance of these domains.

Fig. 5.4 Anion binding site.
Main structural elements that
contribute to the proposed
central anion binding site.
Anions are thought to bind at
a central binding site with
contributions from the
nonhelical segments and the
inward-pointing (N-terminal)
ends of the partial helices of
TMDs 3 and 10
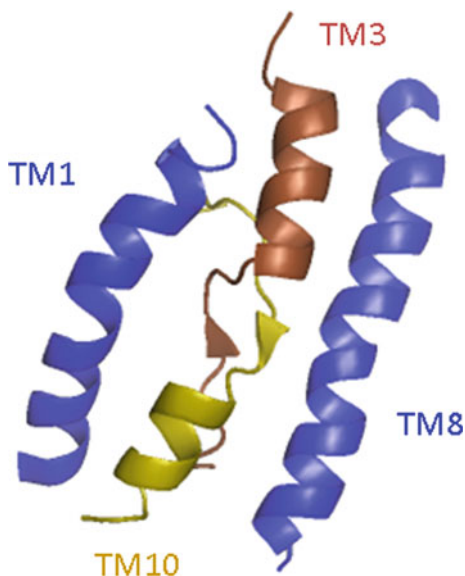
In the crystal structure of the (non-SLC26) transporter UraA, a substrate mole-
cule, uracil, occupies the structurally equivalent central site (Lu et al. 2011).
Although the SLC26Dg crystal structure lacked bound substrate, the high similarity
to UraA and structural details support the identity of the binding site. The dimen-
sions of the cavity in computational and experimental SLC26 structures are com-
patible with the range of the substrate anions accepted by SLC26Dg and prestin,
respectively (Gorbunov et al. 2014; Geertsma et al. 2015). Furthermore, the
N-terminal ends of the partial helices from TM segments 3 and 10 point toward the
binding site from opposite directions, providing likely hydrogen-bond partners for
the substrate (Geertsma et al. 2015; Fig. 5.4). In UraA, a similar arrangement has
been observed, with additional coordination of the substrate by side-chain interac-
tions (Lu et al. 2011). For prestin, Gorbunov et al. (2014) directly tested the role of
the structurally corresponding positions by introducing point mutations. Such
mutations either altered the anion selectivity of prestin, affected the efficacy of the
competitive inhibitory anion salicylate, or abolished function. Similarly, mutations
at the homologous positions in transport-competent prestin orthologs from non-
mammals (chicken; cPres) altered anion selectivity or abolished transport function
(Gorbunov et al. 2014). Altogether, as expected for a transporter, a substrate binding
site is located centrally in SLC26 proteins, including prestin. Importantly, the
mutational analysis suggested that this same binding site not only mediates transport
in SLC26 transporters (including nonmammalian prestin) but also is responsible for
the anion-dependence of eM and NLC mediated by mammalian prestin.

How can these structural findings be reconciled with the functional knowledge
on prestin? Kinetic analysis of the charge movement and motility of prestin indi-
cated that rapid initial binding of a monovalent anion (chloride) is followed by a

slower transition and, subsequently, by the fast voltage-dependent rearrangement that generates both molecular motion and charge movement (Song and Santos-Sacchi 2013). Given that mutating the binding site disrupts prestin function, a plausible conclusion is that the first fast binding step corresponds to the binding of chloride into the SLC26 substrate binding site.

5.3.5 Electromotile Molecular Transitions

Here we consider the prestin structure in the context of the prevailing area-motor model that postulates (at least) two major states with different cross-sectional dimensions. Although this issue awaits its elucidation, some considerations can be made on the basis of the current knowledge.

Functionally, binding of an anion and a subsequent slower conformational transition appear to precede the mechanically productive fast structural rearrangement in mammalian prestin (Oliver et al. 2001; Song and Santos-Sacchi 2013). The concept of molecular rearrangements following binding of an anion into the central substrate binding site shared with other SLC26 homologs (Gorbunov et al. 2014) has been taken to indicate that the mechanical activity of prestin is mechanistically related to the anion transport cycle (Schaechinger et al. 2011; Gorbunov et al. 2014; Geertsma et al. 2015).

In many secondary transporters, substrate translocation occurs via an alternate access mechanism. Thus, a central binding site is alternately exposed to the extra- and intracellular environment, thereby allowing binding of a substrate on one site and dissociation/release at the opposite site of the membrane (Rudnick 2013). Such a mechanism involves at least one major conformational rearrangement and may additionally involve an intermediate occluded state (Fig. 5.5). For some
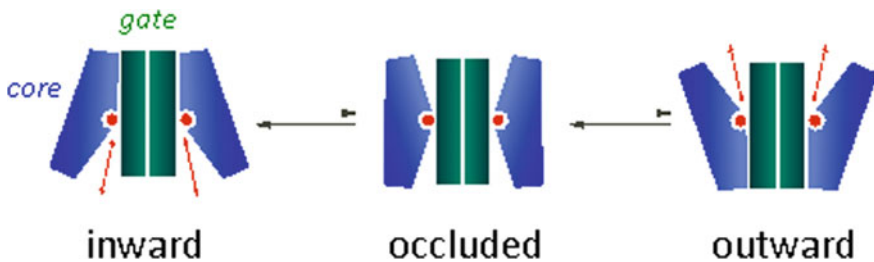

Fig. 5.5 Structural model for anion transport by SLC26. Alternating access of the central anion binding site may result from rotational movement of the core domains against the dimerized gate domains acting as a central scaffold. Experimental crystal structure of SLC26Dg and computational structures of prestin have an inward-facing conformation, but the experimental structure of the structurally homologous exchanger, AE1, revealed an outward-facing conformation (Arakawa et al. 2015). The conformational repertoire of mammalian prestin may be restricted to inward-open and hypothetical occluded states. Modified from Geertsma et al. (2015)

transporters, the conformational change mediating alternate access transport has been structurally resolved. Notably, these transporters also conform to the principle of inverted-repeat architecture, although they are not directly related to SLC26 transporters (Vastermark and Saier 2014). It was shown that there, the conformational switch between inward and outward orientation occurs by a tilting motion between rigid TM bundles (Forrest and Rudnick 2009; Rudnick 2013). For SLC26 transporters, the available structure of SLC26Dg and the UraA-based homology model (as well as the UraA structure itself) describe essentially the same inward-open conformation; therefore, the nature of the molecular rearrangements could not be inferred directly from the structural data (Lu et al. 2011; Gorbunov et al. 2014; Geertsma et al. 2015). However, it has been suggested that a relative motion between core and gate domains mediates transport in SLC26 transporters and UraA (Lu et al. 2011; Gorbunov et al. 2014; Geertsma et al. 2015). Indeed, this idea is strongly supported by the AE1 structure, which revealed an (inhibitor-bound) outside-out state. This structure superposes closely with the UraA and SLC26 structures, with the exception of altered relative positions of core and gate domains (Arakawa et al. 2015). The AE1 structure thus supports the idea of rotation between core and gate domain as the conformational mechanism mediating substrate transport as previously suggested by Gorbunov et al. (2014) and Geertsma et al. (2015; Fig. 5.5). Additional experimental support comes from the finding that a cysteine residue introduced into the central binding site of the transport-active prestin ortholog from chicken is accessible to nonpermeable cysteine-modifying reagents both from the intra- and extracellular sites, consistent with the alternate exposure of this site to both faces of the membrane (Gorbunov et al. 2014).

Given that anion binding into the central binding site in prestin enables eM, it is tempting to speculate that (voltage-dependent) motor activity arises from subsequent conformational transitions equivalent to those mediating anion translocation in other SLC26 transporters (Schaechinger et al. 2011; Gorbunov et al. 2014; Geertsma et al. 2015). In fact, a chimeric SLC26A5 construct based on the zebrafish prestin ortholog ("synthetic prestin") has both electromechanical and transport activity, consistent with the idea that the transport cycle may accommodate transitions that produce eM (Schaechinger et al. 2011). Also, observations on native chicken hair cells suggested that even nonmammalian, i.e., transport-competent, prestin orthologs may be able to generate forces sufficient for motions at the cellular scale (Beurg et al. 2013). However, in contrast to the transport-active prestin orthologs, the central binding of mammalian prestin is exclusively exposed to the intracellular side (Gorbunov et al. 2014), which is consistent with its interaction with anions selectively at the intracellular, cytoplasmic side (Oliver et al. 2001; Rybalchenko and Santos-Sacchi 2003b, 2008). In structural terms, this indicated that mammalian prestin is unable to reach a state where the binding site is fully exposed to the extracellular medium (Schaechinger et al. 2011; Gorbunov et al. 2014). Therefore, if eM arises from structural rearrangements similar to those that mediate anion transport, these states should be equivalent to a segment of the transport cycle from the fully inward-open conformation to a state preceding full exposure to the extracellular face (Schaechinger et al. 2011; Gorbunov et al. 2014).

Another open issue is the molecular nature of the voltage sensitivity of prestin. The steepness of the voltage-induced motility or charge movement suggests that roughly one elementary electrical charge is moved across the electrical field of the membrane to drive electromechanical activity (Santos-Sacchi 1991). Either exchanging the prevalent intracellular monovalent anion (Oliver et al. 2001) or neutralizing the charged amino acids by mutation (Bai et al. 2009) affects the steepness of the voltage dependence of prestin. Accordingly, anions or polar protein domains have been postulated as extrinsic or intrinsic voltage sensors, respectively. Structural identification of the mechanically effective conformational rearrangements should help to identify the molecular nature of the voltage sensor. Understanding the dynamic electromechanical behavior on this structural level will be one of the most fascinating challenges for future work on prestin.

5.4 Interaction of Prestin with Its Cellular Environment

5.4.1 Localization of Prestin Along the Basolateral Wall

After the identification of prestin (Zheng et al. 2000), immunolocalization studies showed the protein along the basolateral surface of OHCs (Belyantseva et al. 2000; Yu et al. 2006). These observations were presaged by electrophysiological localization of motor activity along the lateral membrane (Kalinec et al. 1992; Dallos et al. 1993; Huang and Santos-Sacchi 1993). This localization pattern has important physiological significance because the electromotile force generated by prestin is directed along the longitudinal axis of these elongated cells (Holley and Ashmore 1990; Holley et al. 1992; Matsumoto et al. 2010). It is believed that the unusual structure of the lateral wall of the OHCs, encompassing a prestin-containing plasma membrane, the underlying cortical cytoskeleton, and subsurface cisternae, plays a critical role in eM. The plasma membrane is connected to the underlying cytoskeleton by "pillars," ultrastructurally identified electron-dense entities (Holley and Ashmore 1990; Forge 1991). Nonetheless, the molecular links of prestin to the underlying cytoskeleton are unknown.

The delivery of prestin to the basolateral wall of OHCs has several potential confounding mechanisms. Protein sorting has been best studied in polarized epithelial cells, where work has established a dichotomy of targeting to the apical or basolateral surface. Although hair cells are polarized epithelial cells, they also show properties of neurons, with an apical-receptive area housing the mechanosensitive channels corresponding to a dendritic end and a basal pole housing the synaptic machinery that corresponds to a neuronal axonal end. A long-standing hypothesis first proposed by Dotti and Simons (1990) posited the dendritic end of a neuron to be equivalent to the basolateral surface and the axonal end to correspond to the apical end of polarized epithelial cells. Hair cells, however, confound this neat

division. Thus, hair cells have to be categorized in terms of protein sorting as either epithelial cell-like or neuronal-like.

It has long been established that classic basolateral markers such as β-catenin and Na^+/K^+-ATPase are localized along the basolateral surface of hair cells (Schneider et al. 1987; Leonova and Raphael 1997; Zhang et al. 2015). Zheng et al. (2010) demonstrated that stereociliary proteins, including harmonin and cadherin 23, are targeted to the apical surface of the CL4 cell, a model polarized epithelial cell. The authors also established that prestin was targeted to the basolateral surface of CL4 cells. These data confirm that, at least for these proteins, hair cell protein-sorting mechanisms are akin to those of polarized epithelial cells. Interestingly, using the apically targeted pendrin as a vehicle, Zheng et al. (2010) showed that basolateral targeting of prestin is determined by the C-terminus of prestin. Using site-directed mutagenesis, Zhang et al. (2015) established that two tyrosine residues, Y520 and Y667, are important for targeting prestin to the basolateral surface of polarized MDCK cells. Moreover, these authors demonstrated that this targeting is also dependent on APμ1-B, which is present in hair cells (and epithelial cells) but absent in neuronal cells (Zhang et al. 2015).

5.4.2   Prestin's Interactome

As alluded to in Sect. 5.2, the identity of prestin as the protein responsible for OHC eM has been well established. Recent efforts have also focused on identifying the role of ancillary proteins in the function of prestin. Because prestin has all the molecular features of the motor responsible for eM, this raises the question, Why look for other associated proteins? The response to this lies in three parts. First, in parallel with other systems, in particular ion channels, ancillary proteins modify the biophysical properties of the protein while establishing its localization and transport between different vesicular compartments as well as modifying its rates of turnover. Thus, protein partners may play a similar role with prestin. Second, although many of the biophysical attributes of prestin in OHCs are comparable to those of prestin expressed in heterologous cells, important discrepancies exist (for instance, the V_h of prestin in OHCs lies between −40 and −80 mV, whereas prestin in heterologous cells consistently shows more negative V_h values). Third, although prestin is clearly responsible for eM, there is evidence that links to the underlying cytoskeleton are important for harnessing forces generated by prestin along the longitudinal axis of the cell (Holley and Ashmore 1990; Holley et al. 1992; Matsumoto et al. 2010). How this is brought about is still unknown.

5.4.2.1   Vesicle-Associated Membrane Protein

To date, many proteins that interact with prestin have been identified, although definitive interactions and a clear physiological role have yet to be defined for the

vast majority of these proteins. An initial membrane yeast two-hybrid screen identified several proteins as potential prestin interactors (Zheng et al. 2009). Chief among these interacting proteins were those known for transport between different vesicular compartments. These include vesicle-associated membrane protein, vesicle-associated protein A (VAPA), and Yip1 domain family member 6 (Yipf6; Zheng et al. 2009). Association with VAPA, important for integrity of the endoplasmic reticulum (ER), was found to increase the surface expression of prestin. Interestingly, the effect seemed reciprocal, with decreased amounts of VAPA in prestin-knockout OHCs (Zheng et al. 2009). Although a role for Yipf6 in prestin transport has not been demonstrated, its closest yeast homolog, Yip1p, has been demonstrated to be important for Rab-mediated transport from the ER to the Golgi apparatus (Matern et al. 2000; Barrowman et al. 2003; Spang 2004). Yipf6 mutants have intestinal inflammatory disease, although a clear mechanism has yet to be identified and a hearing phenotype has not yet been defined (Brandl et al. 2012). A second group of proteins (38%) identified by the membrane yeast two-hybrid screen included several mitochondrial membrane proteins (cytochrome *b*, subunits of NADH-ubiquinone oxidoreductase, and ATP synthase 6; Zheng et al. 2009). Mitochondrial proteins are known to be nonspecific interactors in yeast two-hybrid screens. In their screens, mitochondrial proteins were a dominant fraction, and they saw no interactions between mitochondrial proteins and the tip-link protein cadherin 23, arguing against a nonspecific interaction. OHCs from prestin knockouts and knock-in mice with altered voltage sensitivity showed early cell death. Actual measures of mitochondrial dysfunction in prestin knockouts have, however, yet to be demonstrated.

5.4.2.2   Cystic Fibrosis Transmembrane Conductance Regulator

The cystic fibrosis transmembrane conductance regulator (CFTR) was identified by Homma et al. (2010) as interacting with prestin. Interest in the CFTR was piqued because a lateral wall conductance that carries Cl^- has been identified in OHCs (Rybalchenko and Santos-Sacchi 2003b) and because Cl^- is a critical modulator of prestin activity (see Sect. 5.2.5). Like the lateral wall Cl^- conductance, the CFTR also shows mechanosensitivity (Zhang et al. 2010). The CFTR has been shown to interact with a number of other SLC26 family members through their STAS domain (Ko et al. 2004). Although many of these interactions are dependent on PKA phosphorylation of the CFTR R domain, the interactions also result in a mutual activation of CFTR and SLC26 transporter activity (Ko et al. 2004). Homma et al. (2010) convincingly showed interactions between prestin and the CFTR (although the interaction is not dependent on PKA phosphorylation). They also showed that the presence of prestin results in the localization of CFTR from its exclusively apical location to a partial basolateral location in OHCs. Unexpectedly, however, there was little reciprocal functional effect on prestin or the CFTR in OHCs; no effects on NLC or CFTR conductance were observed. In contrast, the interaction in heterologous cells results in enhanced prestin charge movement in response to PKA

activation; a reciprocal enhanced effect on CFTR conductance was not demonstrable in the presence of prestin. Although the findings of the CFTR in the lateral membrane of OHCs in the presence of prestin is intriguing, a physiological role for the CFTR in OHCs has yet to be established. Blockers of CFTR had no effect on OHC lateral wall Cl^- conductance (Rybalchenko and Santos-Sacchi 2003b). Furthermore, mutations of CFTR that causes cystic fibrosis are not associated with hearing defects. Hearing phenotypes in these patients have been well studied, and sensorineural hearing loss was described only in the context of toxic levels of gentamicin that is used for treating repeated pulmonary infections in these patients (Homma et al. 2010).

5.4.2.3   Calmodulin

A recent paper by Keller et al. (2014) identified calmodulin as an interactor of prestin. The identity of calmodulin as an interactor was determined after initial assessments showed intrinsically disordered regions in the C-terminus of prestin in proximity to its STAS domain (Keller et al. 2014). Intrinsically disordered regions have been shown to interact with calmodulin, and Keller et al. (2014) go on to show that prestin binds to calmodulin using these regions in a Ca^{2+}-dependent manner. Importantly, they show a 35-mV shift in V_h with increasing Ca^{2+}, an effect that was reversed by the calmodulin inhibitor trifluoperazine (Keller et al. 2014). The authors then speculate that the Ca^{2+}-induced changes in V_h could have physiological importance, with efferent modulation from the olivocochlear bundle effecting changes in OHC stiffness through increases in Ca^{2+}. These interpretations may not be complete, with changes in V_h induced by Ca^{2+} perfusion being secondary to the effects on turgor pressure and not entirely due to the effects on V_h by a direct effect from calmodulin binding to prestin. Thus, the changes in V_h were not evident when the cells were collapsed before Ca^{2+} perfusion (Song and Santos-Sacchi 2015).

5.4.2.4   Microtubule-Associated Proteins

Microtubule-associated protein 1S (MAP1S) is a protein that was identified as interacting with prestin using a conventional Gal4-based yeast two-hybrid assay (Surguchev et al. 2012). In this assay, the C-terminus of prestin was used as bait. MAP1S is a member of the microtubule-associated protein family. MAP1S coexpression enhanced the surface expression of prestin as established by both biochemical and electrophysiological measures (Surguchev et al. 2012). These findings are paralleled by a gradient of MAP1S mRNA expression along the tonotopic axis, suggesting that MAP1S may bring about the higher amounts of prestin in the plasma membrane of high-frequency hair cells. Interestingly, MAP1S has also been shown to interact with actin, and its concentration in proximity to the lateral wall of OHCs raises the possibility that it serves as the link between prestin and the underlying cytoskeleton. As previously referred to, the lateral wall of OHCs

includes a cortical cytoskeleton sandwiched between subsurface cisternae and the lateral plasma membrane. The cortical cytoskeleton consists of circumferentially arranged actin filaments linked to longitudinally arranged spectrin ($\alpha2$, $\beta5$) filaments (Forge 1991; Kalinec et al. 1992; Legendre et al. 2008). Previous work identified pillars that are electron-dense entities linking OHC lateral membranes to circumferentially arranged actin filaments (Holley and Ashmore 1990; Forge 1991; Kalinec et al. 1992). The molecular composition of pillars is unknown. Because MAP1S also forms a complex with a host of other actin-binding proteins (Liu et al. 2002; Liu and McKeehan 2002), these data raise the possibility that MAP1S is one component of a complex of proteins that form pillar structures.

5.4.2.5 Spectrin and Spectrin-Interacting Proteins

Although prior reports have shown a concentration of two spectrin-interacting proteins (ankyrin or protein 4.1) along the periphery of OHCs (Knipper et al. 1995; Zine and Schweitzer 1997), the wide gap (50 nm) between the cytoskeleton and the lateral membrane makes it unclear whether these proteins have a physiological role or not (Legendre et al. 2008). Moreover, there are no data showing a direct interaction between prestin and ankyrin or protein 4.1. Interestingly, a paper identifying $\beta5$ spectrin as a component of the OHC cytoskeleton showed no interaction between prestin and this spectrin isoform (Legendre et al. 2008). However, these authors found an unknown component in OHC lysates that enabled such an interaction. A key area of research in the future will be exploring the interactions between prestin and other components of the lateral wall.

5.4.2.6 Calcium/Calmodulin-Dependent Serine Protein Kinase

A subsequent study using yeast two-hybrid screens identified calcium/calmodulin-dependent serine protein kinase (CASK) as an interacting partner of prestin (Cimerman et al. 2013). CASK is a membrane-associated guanylate kinase (MAGUK). Members of this family have been shown in other systems to bind membrane proteins linking them to actin through protein 4.1 (Zhu et al. 2016). The subcellular distribution of CASK showed a developmental change that correlated with prestin and was affected by thyroid hormone levels. Normally, by postnatal day (P) 18, both NLC and eM reach mature levels. In hypothyroid animals, there is a delay in the expression of prestin, with NLC levels taking until P28 to reach normal levels. Prestin is normally expressed along the entire basolateral surface early in development and is then localized predominantly along the lateral wall while being largely excluded from the basal pole. In contrast, CASK is found predominantly at the basal pole where OHCs contact Deiters cells. In hypothyroid animals, CASK is expressed at low levels, with prestin expressed over the entire basolateral surface at P28. Coincidentally, although NLC levels were normal, eM responses were markedly reduced. Zhu et al. (2016) reasoned that the interactions

with CASK may be involved in the redistribution of prestin to the lateral wall and in generating force, possibly through the cytoskeleton or OHC interactions with Deiter's cells.

5.4.3 Prestin in the Membrane Environment

It is becoming increasingly appreciated that an interplay of membrane structure, organization, and mechanics regulates the function of membrane proteins. It is thus important to understand how the membrane environment affects the function of prestin. From a thermodynamic point of view, the lipid environment is the "solvent" in which prestin operates, just as water is the solvent for biochemical reactions. Thus, changes in the composition, fluidity, and mechanical properties of the membrane can all affect the molecular function of prestin. At the same time, prestin has a large C-terminus that contains a STAS domain possessing a number of potential protein-protein interaction motifs. It is reasonable to postulate that the STAS domain connects prestin to the cytoskeleton of the cell and places constraints on its mobility. Understanding these supramolecular interactions of prestin is necessary to ultimately understand how the molecular nanoscale events that occur in the prestin protein proper result in the mesoscale rearrangements that must ultimately be responsible for OHC eM.

5.4.3.1 Prestin as a Mechanosensitive Protein

After the original discovery that the membrane capacitance of the OHC was sensitive to membrane stress (Iwasa 1993), the tension sensitivity of prestin was further characterized in both OHCs and HEK cells expressing prestin (Kakehata and Santos-Sacchi 1995; Ludwig et al. 2001; Santos-Sacchi et al. 2001). These studies implied that the application of mechanical force results in a geometric rearrangement in prestin that, in turn, affects its ability to move charge in response to voltage changes, establishing prestin as similar to mechanosensitive channels such as MscL, Piezo1, and TREK1 (Sukharev et al. 1996; Coste et al. 2010; Brohawn et al. 2014). Given that the OHC is under turgor pressure, this mechanical sensitivity is likely to be physiologically important.

The question may be raised as to how prestin senses membrane mechanical forces. Membranes are thin structures that have a large resistance to changes in surface area but a very small resistance to changes in curvature. Curvature stress can be induced by differential partitioning of molecules into the two leaflets of the membrane, corresponding to the classic "bilayer couple" explanation of red blood cell shape changes (Singer and Oster 1992). It has become increasingly appreciated that many mechanosensitive membrane proteins sense mechanical force through the lipid bilayer in accordance with the "force from lipid" principle (Anishkin et al. 2014). Forces may be applied to the lipid bilayer by stretching the area or through

the direct or indirect application of membrane curvature stress. Indeed, many reagents that affect prestin function are also known to change membrane curvature (Oghalai et al. 2000; Brownell et al. 2001). It has been postulated that in the intact OHC, turgor pressure would supply a force leading to nanoscale bending of the membrane between the pillar proteins (Raphael et al. 2000; Spector et al. 2006). Although this is difficult to directly measure in living cells with current technology, measurements using fluorescence polarization microscopy (Greeson and Raphael 2009) are consistent with both the existence of nanoscale curvature and pharmacological-induced changes in this curvature. Specifically, reagents that changed the curvature in opposite directions were found to be consistent with the corresponding changes in the function of prestin as measured by the Boltzmann parameter (V_h) of the NLC (Fang et al. 2007; Greeson and Raphael 2009). Other studies have obtained evidence that prestin is also sensitive to the thickness of the membrane (Fang et al. 2010).

One of the challenges in prestin research has been the lack of pharmacological compounds that inhibit its function. This is an also issue for other mechanosensitive proteins such as MscL (Hamill 2006). The most utilized inhibitor of prestin function is salicylate, an active metabolite of aspirin related to nonsteroidal anti-inflammatory drugs (NSAIDs). NSAIDs and analgesics are associated with ototoxicity, hearing loss, and tinnitus (ringing in the ears). In other membrane proteins, NSAID effects have been attributed to both indirect effects on membrane properties and direct binding to functional regions of proteins (Lichtenberger et al. 2006; Manrique-Moreno et al. 2009). Additional research is needed to identify specific inhibitors of prestin function.

5.4.3.2 Prestin as a Confined Protein

The original fluid-mosaic membrane model proposed that proteins diffuse freely in a sea of lipids (Singer and Nicolson 1972). This picture has been refined by the discovery that different proteins have varying degrees of confinement in the membrane. In the membrane biophysics community, many concepts such as "membrane microdomains" and "lipid rafts" have been espoused to characterize the restricted mobility of membrane proteins. Here, the important questions are, Can prestin diffuse freely or is it constrained? If it is constrained, does this occur through interactions with the cytoskeleton?

The lateral diffusion of prestin was first directly measured using fluorescence recovery after photobleaching (FRAP) in HEK cells expressing prestin (Organ and Raphael 2007). These studies revealed that the diffusion of prestin is relatively slow when compared with proteins of similar molecular weight. In addition, using a dual-bleach protocol, these studies suggested that prestin was transiently confined. To confirm transient confinement and better understand the membrane dynamics of prestin, single-molecule imaging studies were performed (Kamar et al. 2012). Individual molecules of prestin labeled with a highly stable fluorophore were expressed in HEK cells and tracked using total internal fluorescence microscopy.

These studies confirmed that prestin is indeed confined in the membrane and undergoes anomalous diffusion (Kamar et al. 2012). The results could be fit to a "hop-diffusion" model in which prestin molecules diffuse within a limited area, then "hop" to a different area of the membrane. In this model, there is a timescale associated with confinement that corresponds to the strength of the intermolecular interactions restricting free diffusion of the protein. These studies raised the question of how prestin diffuses in the native OHCs. Later studies in knock-in mice expressing prestin fused to yellow fluorescent protein (YFP) obtained results consistent with the minimal diffusion of prestin in OHCs as measured with traditional FRAP (Yamashita et al. 2015). When compared with the HEK cell single-molecule results, it appears that OHCs contain additional mechanisms that further confine prestin (Yamashita et al. 2015). This raises the question whether robust electromechanical activity seen in OHCs as opposed to HEK cells could be related to the presence of additional interactions that limit the membrane lateral mobility of prestin, i.e., whether membrane confinement has implications for prestin function. One of the key ways to alter the confinement of membrane proteins is to manipulate membrane cholesterol, which changes the structure of membrane microdomains. Depletion of membrane cholesterol with MBCD was shown to have a dramatic impact on prestin confinement (Kamar et al. 2012). Taking into account an earlier study that indicated that cholesterol affects the Boltzmann parameter (V_h) of the NLC in OHCs (Rajagopalan et al. 2007), it suggests that alterations in prestin confinement affect at least the operating voltage range of prestin. Similar cholesterol depletion experiments were also carried out in the knock-in mouse model (Yamashita et al. 2015), but here the addition of salicylate was also required to enable prestin to undergo free membrane diffusion. Identifying the molecular mechanisms responsible for prestin confinement and understanding whether they affect prestin function is an important priority for future research.

5.5   Conclusions and Open Questions

Gaining a molecular and cellular understanding of eM function has been the major driving force for the research summarized above. Considering the major advances achieved over the last decade, a mechanistic framework for prestin function is finally emerging.

Only recently have experimental and computational data on the structure of prestin and its relatives been obtained. Yet, these findings already provide unprecedented insights and show remarkable agreement between structure and the wealth of biophysical data assembled since the discovery of eM. This initial structural picture of prestin should now provide a productive ground for well-directed structural and functional approaches toward understanding how molecular conformational dynamics generate eM. Given this goal, it should be kept in mind that the present structural data provide only a snapshot of one particular state, that many structural details are still missing, and, importantly, that the structure of prestin itself

has not been determined experimentally. Thus, much remains to be explored. Additionally, such work may also provide important insights into the inner workings of other SLC26 transporters, including pendrin, another SLC26 member with high relevance for cochlear homeostasis and pathophysiology.

Structure-function results are consistent with the idea that prestin works as a conformationally constrained alternate access transporter (see Fig. 5.5). In such a model, eM would arise from the transition between distinct states within an anion transport cycle that differ mechanically and electrostatically, in turn rendering prestin mechanosensitive. The conformational transition may result in a change of cross-sectional area as proposed by the prevailing area motor model (Iwasa 1994); alternatively, the tilting motion between helical bundles suggested by the available structural data may also indicate the generation of differential stresses between the two leaflets of the membrane bilayer, consistent with a previously proposed membrane bending model of eM based on flexoelectricity (Raphael et al. 2000).

Beyond these molecular mechanisms, many observations suggest that integration of prestin into a complex cellular structure, i.e., the highly specialized trilaminate lateral wall of OHCs, is important for effectively channeling the molecular movements into the generation of macroscopic cellular eM. Yet, components of this cortical structure as well as how it is assembled and whether prestin is part of it remain unknown. Despite identification of various potential interaction partners of prestin described in this chapter, their involvement in the OHC lateral wall and thus their relevance for eM remain unknown. Other important interaction partners likely await identification. Future work on the function of prestin-associated proteins will not only require elucidation of their ultrastructural localization and molecular interactions within the supramolecular OHC cortex but should also include selective manipulation of these proteins and disruption of their interactions in living OHCs.

It can be anticipated that the molecular and supramolecular characterization of prestin will lead to new approaches for selective alteration of eM that can, in turn, increase our overall understanding of the role of eM in cochlear mechanics (i.e., amplification). Ultimately, research along these avenues will increase our understanding of this unique protein that is so important for our sense of hearing.

References

Adachi, M., & Iwasa, K. H. (1999). Electrically driven motor in the outer hair cell: Effect of a mechanical constraint. *Proceedings of the National Academy of Sciences of the United States of America, 96*(13), 7244–7249.

Alper, S. L., & Sharma, A. K. (2013). The SLC26 gene family of anion transporters and channels. *Molecular Aspects of Medicine, 34*(2–3), 494–515.

Anishkin, A., Loukin, S. H., Teng, J., & Kung, C. (2014). Feeling the hidden mechanical forces in lipid bilayer is an original sense. *Proceedings of the National Academy of Sciences of the United States of America,* 111(22), 7898–7905.

Arakawa, T., Kobayashi-Yurugi, T., Alguel, Y., Iwanari, H., Hatae, H., Iwata, M., Abe, Y., Hino, T., Ikeda-Suno, C., Kuma, H., Kang, D., Murata, T., Hamakubo, T., Cameron, A. D., Kobayashi, T., Hamasaki, N., & Iwata, S. (2015). Crystal structure of the anion exchanger domain of human erythrocyte band 3. *Science,* 350(6261), 680–684.

Ashmore, J. (2008). Cochlear outer hair cell motility. *Physiological Reviews,* 88(1), 173–210.

Ashmore, J., Avan, P., Brownell, W. E., Dallos, P., Dierkes, K., Fettiplace, R., Grosh, K., Hackney, C. M., Hudspeth, A. J., Juelicher, F., Lindner, B., Martin, P., Meaud, J., Petit, C., Santos-Sacchi, J. R., & Canlon, B. (2010). The remarkable cochlear amplifier. *Hearing Research,* 266(1–2), 1–17. Corrigendum. *Hearing Research*, 280(1–2), 245.

Ashmore, J. F. (1987). A fast motile response in guinea-pig outer hair cells: The cellular basis of the cochlear amplifier. *The Journal of Physiology,* 388, 323–347.

Ashmore, J. F. (1989). Transducer motor coupling in cochlear outer hair cells. In D. Kemp & J. P. Wilson (Eds.), *Mechanics of Hearing* (pp. 107–113). New York: Plenum Press.

Ashmore, J. F. (1990). Forward and reverse transduction in the mammalian cochlea. *Neuroscience Research Supplement,* 12, S39–S50.

Bai, J. P., Navaratnam, D., Samaranayake, H., & Santos-Sacchi, J. (2006). En block C-terminal charge cluster reversals in prestin (SLC26A5): Effects on voltage-dependent electromechanical activity. *Neuroscience Letters,* 404(3), 270–275.

Bai, J. P., Surguchev, A., Montoya, S., Aronson, P. S., Santos-Sacchi, J., & Navaratnam, D. (2009). Prestin's anion transport and voltage-sensing capabilities are independent. *Biophysical Journal,* 96(8), 3179–3186.

Bai, J. P., Surguchev, A., Ogando, Y., Song, L., Bian, S., Santos-Sacchi, J., & Navaratnam, D. (2010). Prestin surface expression and activity are augmented by interaction with MAP1S, a microtubule-associated protein. *Journal of Biological Chemistry,* 285(27), 20834–20843.

Bai, J.P., Moeini-Naghani, I., Zhong, S., Li, F.Y., Bian, S., Sigworth, F.J., Santos-Sacchi, J., & Navaratnam, D. (2017). Current carried by the Slc26 family member prestin does not flow through the transporter pathway. *Scientific Reports*, 7:46619.

Barrowman, J., Wang, W., Zhang, Y., & Ferro-Novick, S. (2003). The Yip1p•Yif1p complex is required for the fusion competence of endoplasmic reticulum-derived vesicles. *Journal of Biological Chemistry,* 278(22), 19878–19884.

Belyantseva, I. A., Adler, H. J., Curi, R., Frolenkov, G. I., & Kachar, B. (2000). Expression and localization of prestin and the sugar transporter GLUT-5 during development of electromotility in cochlear outer hair cells. *The Journal of Neuroscience,* 20(24), RC116.

Beurg, M., Tan, X., & Fettiplace, R. (2013). A prestin motor in chicken auditory hair cells: Active force generation in a nonmammalian species. *Neuron,* 79(1), 69–81.

Bezanilla, F. (2000). The voltage sensor in voltage-dependent ion channels. *Physiological Reviews,* 80(2), 555–592.

Brandl, K., Tomisato, W., Li, X., Neppl, C., Pirie, E., Falk, W., Xia, Y., Moresco, E. M., Baccala, R., Theofilopoulos, A. N., Schnabl, B., & Beutler, B. (2012). Yip1 domain family, member 6 (Yipf6) mutation induces spontaneous intestinal inflammation in mice. *Proceedings of the National Academy of Sciences of the United States of America,* 109(31), 12650–12655.

Brohawn, S. G., Su, Z., & MacKinnon, R. (2014). Mechanosensitivity is mediated directly by the lipid membrane in TRAAK and TREK1 K$^+$ channels. *Proceedings of the National Academy of Sciences of the United States of America*, 111(9), 3614–3619.

Brownell, W. E., Bader, C. R., Bertrand, D., & de Ribaupierre, Y. (1985). Evoked mechanical responses of isolated cochlear outer hair cells. *Science,* 227(4683), 194–196.

Brownell, W. E., Spector, A. A., Raphael, R. M., & Popel, A. S. (2001). Micro- and nanomechanics of the cochlear outer hair cell. *Annual Review of Biomedical Engineering,* 3, 169–194.

Cimerman, J., Waldhaus, J., Harasztosi, C., Duncker, S. V., Dettling, J., Heidrych, P., Bress, A., Gampe-Braig, C., Frank, G., Gummer, A. W., Oliver, D., Knipper, M., & Zimmermann, U.

(2013). Generation of somatic electromechanical force by outer hair cells may be influenced by prestin-CASK interaction at the basal junction with the Deiter's cell. *Histochemistry and Cell Biology,* 140(2), 119–135.

Compton, E. L., Karinou, E., Naismith, J. H., Gabel, F., & Javelle, A. (2011). Low resolution structure of a bacterial SLC26 transporter reveals dimeric stoichiometry and mobile intracellular domains. *Journal of Biological Chemistry,* 286(30), 27058–27067.

Compton, E. L., Page, K., Findlay, H. E., Haertlein, M., Moulin, M., Zachariae, U., Norman, D. G., Gabel, F., & Javelle, A. (2014). Conserved structure and domain organization among bacterial Slc26 transporters. *Biochemical Journal,* 463(2), 297–307.

Coste, B., Mathur, J., Schmidt, M., Earley, T. J., Ranade, S., Petrus, M. J., Dubin, A. E., & Patapoutian, A. (2010). Piezo1 and Piezo2 are essential components of distinct mechanically activated cation channels. *Science*, 330(6000), 55–60.

Dallos, P., & Evans, B. N. (1995). High-frequency motility of outer hair cells and the cochlear amplifier. *Science,* 267(5206), 2006–2009.

Dallos, P., Evans, B. N., & Hallworth, R. (1991). Nature of the motor element in electrokinetic shape changes of cochlear outer hair cells. *Nature, 350*(6314), 155–157.

Dallos, P., Hallworth, R., & Evans, B. N. (1993). Theory of electrically driven shape changes of cochlear outer hair cells. *Journal of Neurophysiology,* 70(1), 299–323.

Dallos, P., Wu, X., Cheatham, M. A., Gao, J., Zheng, J., Anderson, C. T., Jia, S., Wang, X., Cheng, W. H., Sengupta, S., He, D. Z., & Zuo, J. (2008). Prestin-based outer hair cell motility is necessary for mammalian cochlear amplification. *Neuron,* 58(3), 333–339.

Deak, L., Zheng, J., Orem, A., Du, G. G., Aguinaga, S., Matsuda, K., & Dallos, P. (2005). Effects of cyclic nucleotides on the function of prestin. *The Journal of Physiology,* 563(2), 483–496.

Detro-Dassen, S., Schanzler, M., Lauks, H., Martin, I., zu Berstenhorst, S. M., Nothmann, D., Torres-Salazar, D., Hidalgo, P., Schmalzing, G., & Fahlke, C. (2008). Conserved dimeric subunit stoichiometry of SLC26 multifunctional anion exchangers. *Journal of Biological Chemistry,* 283(7), 4177–4188.

Dorwart, M. R., Shcheynikov, N., Yang, D., & Muallem, S. (2008). The solute carrier 26 family of proteins in epithelial ion transport. *Physiology,* 23, 104–114.

Dotti, C. G., & Simons, K. (1990). Polarized sorting of viral glycoproteins to the axon and dendrites of hippocampal neurons in culture. *Cell,* 62(1), 63–72.

Fang, J., & K. H. Iwasa. (2007). Effects of chlorpromazine and trinitrophenol on the membrane motor of outer hair cells. *Biophysical journal*, 93:1809–1817.

Fang, J., Izumi, C., & Iwasa, K. H. (2010). Sensitivity of prestin-based membrane motor to membrane thickness. *Biophysical Journal,* 98(12), 2831–2838.

Finn, R. D., Bateman, A., Clements, J., Coggill, P., Eberhardt, R. Y., Eddy, S. R., Heger, A., Hetherington, K., Holm, L., Mistry, J., Sonnhammer, E. L., Tate, J., & Punta, M. (2014). Pfam: The protein families database. *Nucleic Acids Research,* 42, D222–D230.

Fisher, J. A., Nin, F., Reichenbach, T., Uthaiah, R. C., & Hudspeth, A. J. (2012). The spatial pattern of cochlear amplification. *Neuron,* 76(5), 989–997.

Forge, A. (1991). Structural features of the lateral walls in mammalian cochlear outer hair cells. *Cell and Tissue Research,* 265(3), 473–483.

Forrest, L. R., & Rudnick, G. (2009). The rocking bundle: A mechanism for ion-coupled solute flux by symmetrical transporters. *Physiology,* 24, 377–386.

Frank, G., Hemmert, W., & Gummer, A. W. (1999). Limiting dynamics of high-frequency electromechanical transduction of outer hair cells. *Proceedings of the National Academy of Sciences of the United States of America,* 96(8), 4420–4425.

Gale, J. E., & Ashmore, J. F. (1994). Charge displacement induced by rapid stretch in the basolateral membrane of the guinea-pig outer hair cell. *Proceedings of the Royal Society of London B: Biological Sciences,* 255(1344), 243–249.

Gale, J. E., & Ashmore, J. F. (1997a). The outer hair cell motor in membrane patches. *Pflügers Archiv - European Journal of Physiology,* 434(3), 267–271.

Gale, J. E., & Ashmore, J. F. (1997b). An intrinsic frequency limit to the cochlear amplifier. *Nature,* 389(6646), 63–66.

Geertsma, E. R., Chang, Y. N., Shaik, F. R., Neldner, Y., Pardon, E., Steyaert, J., & Dutzler, R. (2015). Structure of a prokaryotic fumarate transporter reveals the architecture of the SLC26 family. *Nature Structural & Molecular Biology, 22*, 803–808.

Gorbunov, D., Sturlese, M., Nies, F., Kluge, M., Bellanda, M., Battistutta, R., & Oliver, D. (2014). Molecular architecture and the structural basis for anion interaction in prestin and SLC26 transporters. *Nature Communications, 5*, 3622.

Greeson, J. N., & Raphael, R. M. (2009). Amphipath-induced nanoscale changes in outer hair cell plasma membrane curvature. *Biophysical Journal, 96*(2), 510–520.

Hallworth, R., & Nichols, M. G. (2012). Prestin in HEK cells is an obligate tetramer. *Journal of Neurophysiology, 107*(1), 5–11.

Hamill, O. P. (2006). Twenty odd years of stretch-sensitive channels. *Pflügers Archiv - European Journal of Physiology*, 453(3), 333–351.

He, D. Z., Zheng, J., Kalinec, F., Kakehata, S., & Santos-Sacchi, J. (2006). Tuning into the amazing outer hair cell: Membrane wizardry with a twist and shout. *Journal of Membrane Biology, 209*(2–3), 119–134.

Hoglund, P. J., Nordstrom, K. J., Schioth, H. B., & Fredriksson, R. (2011). The solute carrier families have a remarkably long evolutionary history with the majority of the human families present before divergence of bilaterian species. *Molecular Biology and Evolution, 28*(4), 1531–1541.

Holley, M. C., & Ashmore, J. F. (1990). Spectrin, actin and the structure of the cortical lattice in mammalian cochlear outer hair cells. *Journal of Cell Science, 96*(2), 283–291.

Holley, M. C., Kalinec, F., & Kachar, B. (1992). Structure of the cortical cytoskeleton in mammalian outer hair cells. *Journal of Cell Science, 102*(3), 569–580.

Homma, K., Miller, K. K., Anderson, C. T., Sengupta, S., Du, G. G., Aguinaga, S., Cheatham, M., Dallos, P., & Zheng, J. (2010). Interaction between CFTR and prestin (SLC26A5). *Biochimica et Biophysica Acta, 1798*(6), 1029–1040.

Homma, K., Duan, C., Zheng, J., Cheatham, M. A., & Dallos, P. (2013). The V499G/Y501H mutation impairs fast motor kinetics of prestin and has significance for defining functional independence of individual prestin subunits. *Journal of Biological Chemistry, 288*(4), 2452–2463.

Huang, G., & Santos-Sacchi, J. (1993). Mapping the distribution of the outer hair cell motility voltage sensor by electrical amputation. *Biophysical Journal, 65*(5), 2228–2236.

Huang, G. J., & Santos-Sacchi, J. (1994). Motility voltage sensor of the outer hair cell resides within the lateral plasma-membrane. *Proceedings of the National Academy of Sciences of the United States of America, 91*(25), 12268–12272.

Iwasa, K. H. (1993). Effect of stress on the membrane capacitance of the auditory outer hair cell. *Biophysical Journal, 65*(1), 492–498.

Iwasa, K. H. (1994). A membrane motor model for the fast motility of the outer hair cell. *The Journal of the Acoustical Society of America, 96*(4), 2216–2224.

Kachar, B., Brownell, W. E., Altschuler, R., & Fex, J. (1986). Electrokinetic shape changes of cochlear outer hair cells. *Nature, 322*(6077), 365–368.

Kakehata, S., & Santos-Sacchi, J. (1995). Membrane tension directly shifts voltage dependence of outer hair cell motility and associated gating charge. *Biophysical Journal, 68*(5), 2190–2197.

Kakehata, S., & Santos-Sacchi, J. (1996). Effects of salicylate and lanthanides on outer hair cell motility and associated gating charge. *The Journal of Neuroscience, 16*(16), 4881–4889.

Kalinec, F., Holley, M. C., Iwasa, K. H., Lim, D. J., & Kachar, B. (1992). A membrane-based force generation mechanism in auditory sensory cells. *Proceedings of the National Academy of Sciences of the United States of America, 89*(18), 8671–8675.

Kamar, R. I., Organ-Darling, L. E., & Raphael, R. M. (2012). Membrane cholesterol strongly influences confined diffusion of prestin. *Biophysical Journal, 103*(8), 1627–1636.

Keller, J. P., Homma, K., Duan, C., Zheng, J., Cheatham, M. A., & Dallos, P. (2014). Functional regulation of the SLC26-family protein prestin by calcium/calmodulin. *The Journal of Neuroscience, 34*(4), 1325–1332.

Knipper, M., Zimmermann, U., Kopschall, I., Rohbock, K., Jungling, S., & Zenner, H. P. (1995). Immunological identification of candidate proteins involved in regulating active shape changes of outer hair cells. *Hearing Research, 86*(1–2), 100–110.

Ko, S. B., Zeng, W., Dorwart, M. R., Luo, X., Kim, K. H., Millen, L., Goto, H., Naruse, S., Soyombo, A., Thomas, P. J., & Muallem, S. (2004). Gating of CFTR by the STAS domain of SLC26 transporters. *Nature Cell Biology, 6*(4), 343–350.

Legendre, K., Safieddine, S., Kussel-Andermann, P., Petit, C., & El-Amraoui, A. (2008). αII-βV spectrin bridges the plasma membrane and cortical lattice in the lateral wall of the auditory outer hair cells. *Journal of Cell Science, 121*(20), 3347–3356.

Leonova, E. V., & Raphael, Y. (1997). Organization of cell junctions and cytoskeleton in the reticular lamina in normal and ototoxically damaged organ of Corti. *Hearing Research, 113*(1–2), 14–28.

Li, Y., Liu, Z., Shi, P., & Zhang, J. (2010). The hearing gene prestin unites echolocating bats and whales. *Current Biology, 20*(2), R55–R56.

Liberman, M. C., Gao, J., He, D. Z., Wu, X., Jia, S., & Zuo, J. (2002). Prestin is required for electromotility of the outer hair cell and for the cochlear amplifier. *Nature, 419*(6904), 300–304.

Lichtenberger, L. M., Zhou, Y., Dial, E. J., & Raphael, R. M. (2006). NSAID injury to the gastrointestinal tract: Evidence that NSAIDs interact with phospholipids to weaken the hydrophobic surface barrier and induce the formation of unstable pores in membranes. *Journal of Pharmacy and Pharmacology, 58*(11), 1421–1428.

Liu, L., & McKeehan, W. L. (2002). Sequence analysis of LRPPRC and its SEC1 domain interaction partners suggests roles in cytoskeletal organization, vesicular trafficking, nucleo-cytosolic shuttling, and chromosome activity. *Genomics, 79*(1), 124–136.

Liu, L., Amy, V., Liu, G., & McKeehan, W. L. (2002). Novel complex integrating mitochondria and the microtubular cytoskeleton with chromosome remodeling and tumor suppressor RASSF1 deduced by in silico homology analysis, interaction cloning in yeast, and colocalization in cultured cells. *In Vitro Cellular & Developmental Biology - Animal, 38*(10), 582–594.

Liu, Y., Cotton, J. A., Shen, B., Han, X., Rossiter, S. J., & Zhang, S. (2010). Convergent sequence evolution between echolocating bats and dolphins. *Current Biology, 20*(2), R53–R54.

Liu, Z., Qi, F. Y., Zhou, X., Ren, H. Q., & Shi, P. (2014). Parallel sites implicate functional convergence of the hearing gene prestin among echolocating mammals. *Molecular Biology and Evolution, 31*(9), 2415–2424.

Lolli, G., Pasqualetto, E., Costanzi, E., Bonetto, G., & Battistutta, R. (2015). The STAS domain of mammalian SLC26A5 prestin harbors an anion-binding site. *Biochemical Journal, 473*(4), 365–370.

Lovas, S., He, D. Z., Liu, H., Tang, J., Pecka, J. L., Hatfield, M. P., & Beisel, K. W. (2015). Glutamate transporter homolog-based model predicts that anion-π interaction is the mechanism for the voltage-dependent response of prestin. *Journal of Biological Chemistry, 290*(40), 24326–24339.

Lu, F., Li, S., Jiang, Y., Jiang, J., Fan, H., Lu, G., Deng, D., Dang, S., Zhang, X., Wang, J., & Yan, N. (2011). Structure and mechanism of the uracil transporter UraA. *Nature, 472*(7342), 243–246.

Ludwig, J., Oliver, D., Frank, G., Klöcker, N., Gummer, A. W., & Fakler, B. (2001). Reciprocal electromechanical properties of rat prestin: The motor molecule from rat outer hair cells. *Proceedings of the National Academy of Sciences of the United States of America, 98*(7), 4178–4183.

Mahendrasingam, S., Beurg, M., Fettiplace, R., & Hackney, C. M. (2010). The ultrastructural distribution of prestin in outer hair cells: A post-embedding immunogold investigation of low-frequency and high-frequency regions of the rat cochlea. *European Journal of Neuroscience, 31*(9), 1595–1605.

Manrique-Moreno, M., Garidel, P., Suwalsky, M., Howe, J., & Brandenburg, K. (2009). The membrane-activity of ibuprofen, diclofenac, and naproxen: A physico-chemical study with lecithin phospholipids. *Biochimica et Biophysica Acta*, 1788(6), 1296–1303.

Matern, H., Yang, X., Andrulis, E., Sternglanz, R., Trepte, H. H., & Gallwitz, D. (2000). A novel Golgi membrane protein is part of a GTPase-binding protein complex involved in vesicle targeting. *The EMBO Journal,* 19(17), 4485–4492.

Matsumoto, N., Kitani, R., Maricle, A., Mueller, M., & Kalinec, F. (2010). Pivotal role of actin depolymerization in the regulation of cochlear outer hair cell motility. *Biophysical Journal,* 99(7), 2067–2076.

Meltzer, J., & Santos-Sacchi, J. (2001). Temperature dependence of non-linear capacitance in human embryonic kidney cells transfected with prestin, the outer hair cell motor protein. *Neuroscience Letters,* 313(3), 141–144.

Mio, K., Kubo, Y., Ogura, T., Yamamoto, T., Arisaka, F., & Sato, C. (2008). The motor protein prestin is a bullet-shaped molecule with inner cavities. *Journal of Biological Chemistry,* 283(2), 1137–1145.

Mistrik, P., Daudet, N., Morandell, K., & Ashmore, J. F. (2012). Mammalian prestin is a weak Cl^-/HCO_3^- electrogenic antiporter. *The Journal of Physiology,* 590(22), 5597–5610.

Mount, D. B., & Romero, M. F. (2004). The SLC26 gene family of multifunctional anion exchangers. *Pflügers Archiv - European Journal of Physiology,* 447(5), 710–721.

Muallem, D., & Ashmore, J. (2006). An anion antiporter model of prestin, the outer hair cell motor protein. *Biophysical Journal,* 90(11), 4035–4045.

Mutai, H., Suzuki, N., Shimizu, A., Torii, C., Namba, K., Morimoto, N., Kudoh, J., Kaga, K., Kosaki, K., & Matsunaga, T. (2013). Diverse spectrum of rare deafness genes underlies early-childhood hearing loss in japanese patients: A cross-sectional, multi-center next-generation sequencing study. *Orphanet Journal of Rare Diseases,* 8, 172.

Navaratnam, D., Bai, J. P., Samaranayake, H., & Santos-Sacchi, J. (2005). N-terminal-mediated homomultimerization of prestin, the outer hair cell motor protein. *Biophysical Journal,* 89(5), 3345–3352.

Oghalai, J. S., Zhao, H. B., Kutz, J. W., & Brownell, W. E. (2000). Voltage- and tension-dependent lipid mobility in the outer hair cell plasma membrane. *Science,* 287(5453), 658–661.

Ohana, E., Shcheynikov, N., Yang, D., So, I., & Muallem, S. (2011). Determinants of coupled transport and uncoupled current by the electrogenic SLC26 transporters. *The Journal of General Physiology,* 137(2), 239–251.

Oliver, D., He, D. Z., Klocker, N., Ludwig, J., Schulte, U., Waldegger, S., Ruppersberg, J. P., Dallos, P., & Fakler, B. (2001). Intracellular anions as the voltage sensor of prestin, the outer hair cell motor protein. *Science,* 292(5525), 2340–2343.

Organ, L. E., & Raphael, R. M. (2007). Application of fluorescence recovery after photobleaching to study prestin lateral mobility in the human embryonic kidney cell. *Journal of Biomedical Optics,* 12(2), 021003.

Pasqualetto, E., Aiello, R., Gesiot, L., Bonetto, G., Bellanda, M., & Battistutta, R. (2010). Structure of the cytosolic portion of the motor protein prestin and functional role of the STAS domain in SLC26/SulP anion transporters. *Journal of Molecular Biology,* 400(3), 448–462.

Rajagopalan, L., Patel, N., Madabushi, S., Goddard, J. A., Anjan, V., Lin, F., Shope, C., Farrell, B., Lichtarge, O., Davidson, A. L., Brownell, W. E., & Pereira, F. A. (2006). Essential helix interactions in the anion transporter domain of prestin revealed by evolutionary trace analysis. *The Journal of Neuroscience,* 26(49), 12727–12734.

Rajagopalan, L., Greeson, J. N., Xia, A., Liu, H., Sturm, A., Raphael, R. M., Davidson, A. L., Oghalai, J. S., Pereira, F. A., & Brownell, W. E. (2007). Tuning of the outer hair cell motor by membrane cholesterol. *Journal of Biological Chemistry,* 282(50), 36659–36670.

Raphael, R. M., Popel, A. S., & Brownell, W. E. (2000). A membrane bending model of outer hair cell electromotility. *Biophysical Journal,* 78(6), 2844–2862.

Rudnick, G. (2013). How do transporters couple solute movements? *Molecular Membrane Biology,* 30(7), 355–359.

Rybalchenko, V., & Santos-Sacchi, J. (2003a). Allosteric modulation of the outer hair cell motor protein prestin by chloride. In A. Gummer (Ed.), *Biophysics of the Cochlea: From Molecules to Models* (pp. 116–126). Singapore: World Scientific Publishing.

Rybalchenko, V., & Santos-Sacchi, J. (2003b). Cl⁻ flux through a non-selective, stretch-sensitive conductance influences the outer hair cell motor of the guinea-pig. *The Journal of Physiology, 547*(3), 873–891.

Rybalchenko, V., & Santos-Sacchi, J. (2008). Anion control of voltage sensing by the motor protein prestin in outer hair cells. *Biophysical Journal, 95*(9), 4439–4447.

Saier, M. H., Jr., Eng, B. H., Fard, S., Garg, J., Haggerty, D. A., Hutchinson, W. J., Jack, D. L., Lai, E. C., Liu, H. J., Nusinew, D. P., Omar, A. M., Pao, S. S., Paulsen, I. T., Quan, J. A., Sliwinski, M., Tseng, T. T., Wachi, S., & Young, G. B. (1999). Phylogenetic characterization of novel transport protein families revealed by genome analyses. *Biochimica et Biophysica Acta, 1422*(1), 1–56.

Santos-Sacchi, J. (1989). Asymmetry in voltage-dependent movements of isolated outer hair cells from the organ of Corti. *The Journal of Neuroscience, 9*(8), 2954–2962.

Santos-Sacchi, J. (1990). Fast outer hair cell motility: How fast is fast? In P. Dallos, C. D. Geisler, J. W. Matthews, M. A. Ruggero, & C. R. Steele (Eds.), *The Mechanics and Biophysics of Hearing* (pp. 69–75). Berlin: Springer-Verlag.

Santos-Sacchi, J. (1991). Reversible inhibition of voltage-dependent outer hair cell motility and capacitance. *The Journal of Neuroscience, 11*(10), 3096–3110.

Santos-Sacchi, J. (1992). On the frequency limit and phase of outer hair cell motility: Effects of the membrane filter. *The Journal of Neuroscience, 12*(5), 1906–1916.

Santos-Sacchi, J. (1993). Harmonics of outer hair cell motility. *Biophysical Journal, 65*(5), 2217–2227.

Santos-Sacchi, J., & Dilger, J. P. (1988). Whole cell currents and mechanical responses of isolated outer hair cells. *Hearing Research, 35*(2–3), 143–150.

Santos-Sacchi, J., & Huang, G. J. (1998). Temperature dependence of outer hair cell nonlinear capacitance. *Hearing Research, 116*(1–2), 99–106.

Santos-Sacchi, J., & Navarrete, E. (2002). Voltage-dependent changes in specific membrane capacitance caused by prestin, the outer hair cell lateral membrane motor. *Pflügers Archiv - European Journal of Physiology, 444*(1–2), 99–106.

Santos-Sacchi, J., & Song, L. (2014a). Chloride and salicylate influence prestin-dependent specific membrane capacitance. *Journal of Biological Chemistry, 289*(15), 10823–10830.

Santos-Sacchi, J., & Song, L. (2014b). Chloride-driven electromechanical phase lags at acoustic frequencies are generated by SLC26a5, the outer hair cell motor protein. *Biophysical Journal, 107*(1), 126–133.

Santos-Sacchi, J., & Song, L. (2016). Chloride anions regulate kinetics but not voltage-sensor Q_{max} of the solute carrier SLC26a5. *Biophysical Journal, 110*, 1–11.

Santos-Sacchi, J., Kakehata, S., & Takahashi, S. (1998). Effects of membrane potential on the voltage dependence of motility-related charge in outer hair cells of the guinea-pig. *The Journal of Physiology, 510*(1), 225–235.

Santos-Sacchi, J., Shen, W., Zheng, J., & Dallos, P. (2001). Effects of membrane potential and tension on prestin, the outer hair cell lateral membrane motor protein. *The Journal of Physiology, 531*(3), 661–666.

Santos-Sacchi, J., Song, L., Zheng, J. F., & Nuttall, A. L. (2006). Control of mammalian cochlear amplification by chloride anions. *The Journal of Neuroscience, 26*(15), 3992–3998.

Schaechinger, T. J., & Oliver, D. (2007). Nonmammalian orthologs of prestin (SLC26A5) are electrogenic divalent/chloride anion exchangers. *Proceedings of the National Academy of Sciences of the United States of America, 104*(18), 7693–7698.

Schaechinger, T. J., Gorbunov, D., Halaszovich, C. R., Moser, T., Kugler, S., Fakler, B., & Oliver, D. (2011). A synthetic prestin reveals protein domains and molecular operation of outer hair cell piezoelectricity. *The EMBO Journal, 30*(14), 2793–2804.

Schanzler, M., & Fahlke, C. (2012). Anion transport by the cochlear motor protein prestin. *The Journal of Physiology, 590*(2), 259–272.

Scherer, M. P., & Gummer, A. W. (2005). How many states can the motor molecule, prestin, assume in an electric field? *Biophysical Journal: Biophysical Letters*, 88(5), L27–L29.

Schneider, M. E., Cotanche, D. A., Fambrough, D. M., Saunders, J. C., & Matschinsky, F. M. (1987). Immunocytochemical and quantitative studies of Na^+,K^+-ATPase distribution in the developing chick cochlea. *Hearing Research,* 31(1), 39–53.

Sharma, A. K., Rigby, A. C., & Alper, S. L. (2011). STAS domain structure and function. *Cellular Physiology and Biochemistry,* 28(3), 407–422.

Singer, S. J., & Nicolson, G. L. (1972). The fluid mosaic model of the structure of cell membranes. *Science,* 175(4023), 720–731.

Singer, S. J., & Oster, G. F. (1992). The bilayer couple hypothesis. *Trends in Cell Biology*, 2(3), 69–70.

Song, L., & Santos-Sacchi, J. (2010). Conformational state-dependent anion binding in prestin: Evidence for allosteric modulation. *Biophysical Journal,* 98(3), 371–376.

Song, L., & Santos-Sacchi, J. (2013). Disparities in voltage-sensor charge and electromotility imply slow chloride-driven state transitions in the solute carrier SLC26a5. *Proceedings of the National Academy of Sciences of the United States of America,* 110(10), 3883–3888.

Song, L., & Santos-Sacchi, J. (2015). Intracellular calcium affects prestin's voltage operating point indirectly via turgor-induced membrane tension. In K. D. Karavitaki & D. P. Corey (Eds.), *Mechanics of Hearing: Protein to Perception: Proceedings of the 12th International Workshop on the Mechanics of Hearing,* Cape Sounio, Greece, June 23–29, 2014. Melville, NY: American Institute of Physics Conference Proceedings 1703, 030009.

Spang, A. (2004). Vesicle transport: A close collaboration of Rabs and effectors. *Current Biology,* 14(1), R33–R34.

Spector, A. A., Deo, N., Grosh, K., Ratnanather, J. T., & Raphael, R. M. (2006). Electromechanical models of the outer hair cell composite membrane. *Journal of Membrane Biology,* 209(2–3), 135–152.

Sukharev, S. I., Blount, P., Martinac, B., Guy, H. R., & Kung, C. (1996). MscL: A mechanosensitive channel in *Escherichia coli*. *Society of General Physiologists Series*, 51, 133–141.

Surguchev, A., Bai, J. P., Joshi, P., & Navaratnam, D. (2012). Hair cell BK channels interact with RACK1, and PKC increases its expression on the cell surface by indirect phosphorylation. *American Journal of Physiology - Cell Physiology,* 303(2), C143–C150.

Tan, X., Pecka, J. L., Tang, J., Okoruwa, O. E., Zhang, Q., Beisel, K. W., & He, D. Z. (2011). From zebrafish to mammal: Functional evolution of prestin, the motor protein of cochlear outer hair cells. *Journal of Neurophysiology,* 105(1), 36–44.

Tunstall, M. J., Gale, J. E., & Ashmore, J. F. (1995). Action of salicylate on membrane capacitance of outer hair cells from the guinea-pig cochlea. *The Journal of Physiology,* 485(3), 739–752.

Vastermark, A., & Saier, M. H. (2014). Evolutionary relationship between 5 + 5 and 7 + 7 inverted repeat folds within the amino acid-polyamine-organocation superfamily. *Proteins: Structure, Function, and Bioinformatics,* 82(2), 336–346.

Wong, F. H., Chen, J. S., Reddy, V., Day, J. L., Shlykov, M. A., Wakabayashi, S. T., & Saier, M. H., Jr. (2012). The amino acid-polyamine-organocation superfamily. *Journal of Molecular Microbiology and Biotechnology,* 22(2), 105–113.

Yamashita, T., Hakizimana, P., Wu, S., Hassan, A., Jacob, S., Temirov, J., Fang, J., Mellado-Lagarde, M., Gursky, R., Horner, L., Leibiger, B., Leijon, S., Centonze, V. E., Berggren, P. O., Frase, S., Auer, M., Brownell, W. E., Fridberger, A., & Zuo, J. (2015). Outer hair cell lateral wall structure constrains the mobility of plasma membrane proteins. *PLoS Genetics,* 11(9), e1005500.

Yu, N., Zhu, M. L., & Zhao, H. B. (2006). Prestin is expressed on the whole outer hair cell basolateral surface. *Brain Research,* 1095(1), 51–58.

Zhang, W. K., Wang, D., Duan, Y., Loy, M. M., Chan, H. C., & Huang, P. (2010). Mechanosensitive gating of CFTR. *Nature Cell Biology,* 12(5), 507–512.

Zhang, Y., Moeini-Naghani, I., Bai, J., Santos-Sacchi, J., & Navaratnam, D. S. (2015). Tyrosine motifs are required for prestin basolateral membrane targeting. *Biology Open,* 4(2), 197–205.

Zheng, J., Shen, W., He, D. Z., Long, K. B., Madison, L. D., & Dallos, P. (2000). Prestin is the motor protein of cochlear outer hair cells. *Nature, 405*(6783), 149–155.

Zheng, J., Long, K. B., Shen, W., Madison, L. D., & Dallos, P. (2001). Prestin topology: Localization of protein epitopes in relation to the plasma membrane. *NeuroReport, 12*(9), 1929–1935.

Zheng, J., Du, G. G., Matsuda, K., Orem, A., Aguinaga, S., Deak, L., Navarrete, E., Madison, L. D., & Dallos, P. (2005). The C-terminus of prestin influences nonlinear capacitance and plasma membrane targeting. *Journal of Cell Science, 118*(13), 2987–2996.

Zheng, J., Du, G. G., Anderson, C. T., Keller, J. P., Orem, A., Dallos, P., & Cheatham, M. (2006). Analysis of the oligomeric structure of the motor protein prestin. *Journal of Biological Chemistry, 281*(29), 19916–19924.

Zheng, J., Anderson, C. T., Miller, K. K., Cheatham, M., & Dallos, P. (2009). Identifying components of the hair cell interactome involved in cochlear amplification. *BMC Genomics, 10*, 127.

Zheng, L., Zheng, J., Whitlon, D. S., Garcia-Añoveros, J., & Bartles, J. R. (2010). Targeting of the hair cell proteins cadherin 23, harmonin, myosin XVa, espin, and prestin in an epithelial cell model. *The Journal of Neuroscience, 30*(21), 7187–7201.

Zhu, J., Shang, Y., & Zhang, M. (2016). Mechanistic basis of MAGUK-organized complexes in synaptic development and signalling. *Nature Reviews Neuroscience, 17*(4), 209–223.

Zine, A., & Schweitzer, L. (1997). Localization of proteins associated with the outer hair cell plasma membrane in the gerbil cochlea. *Neuroscience, 80*(4), 1247–1254.